Supplementary Information

Quasi-Solid State Nanoparticle/(Ionic Liquid) Gels with Significantly High Ionic Thermoelectric Properties

Xu He,[a] Hanlin Cheng[a,*], Shizhong Yue[a], Jianyong Ouyang[a,*]

[a] Department of Materials Science and Engineering, National University of Singapore, 117576, Singapore

* Corresponding authors at: Department of Materials Science and Engineering, National University of Singapore, 117576, Singapore

Email: mseoj@nus.edu.sg (J. Ouyang), msech@nus.edu.sg (H. Cheng)

Materials

SiO_2 nanoparticles (fumed silicas) with average sizes of 7, 14 and 500 nm were purchased from Sigma-Aldrich Co., SiO_2 nanoparticles with an average size of 20 nm were purchased from Aerosil Co., and SiO_2 nanoparticles with an average size of 30 nm were obtained from EPRUI Biotech Co. Ltd. All silica samples were dried at 120 °C for 10 h before use. Three ionic liquids, 1-ethyl-3-methylimidazolium dicyanamide (EMIM-DCA, ≥98%) 1-ethyl-3-methylimidazolium tetrafluoroborate (EMIM-BF_4, ≥98%) and 1-ethyl-3-methylimidazolium bis(trifluoromethylsulfonyl)imide (EMIM-TFSI, ≥98%), were obtained from Sigma-Aldrich Co. Conductive silver (Ag) paste was supplied by Ted Pella (Pelco). Single-walled carbon nanotubes (SWCNTs, Timesnano) were purchased from Chengdu Organic Chemistry Co. Ltd.

Preparation of ionogels and fabrication of ITESCs

The ionogels were prepared by grounding silica with ionic liquid in an agate mortar for at least 30 min. The samples for the Seebeck coefficient measurement were prepared by casting ionogels on glass substrate coated with Ag electrodes. The Ag electrodes with a length of 13 mm were prepared by screen printing the Pelco Ag paste. The size of glass substrate is 1.3 × 2.6 cm^2. Mixtures of EMIM-DCA and SiO_2 nanoparticles with an average size of 20 nm were mainly studied unless otherwise denoted.

To fabricate an ITESC, Ag strips with a thickness of 10 μm and area of 1.5×1.5 cm^2 were firstly coated on glass substrate. Then, an 8 μm-thick SWCNT layer were deposited on each Ag strip by dropping an aqueous dispersion consisted of 2 mg mL^{-1} SWCNTs and 5 mg mL^{-1} sodium dodecyl

sulfate (SDS). After dried at room temperature for 12 hrs, the SWCNT electrodes were washed with DI water and then dried at 100 ˚C for 30 min. The ITESC was fabricated by placing two SWCNT electrodes face to face with a gap of 1 mm controlled by spacer. The space between the two electrodes was filled with an ionogel. Finally, the as-prepared supercapacitor was sealed with epoxy glue for measurement.

Characterizations

The ionic Seebeck coeffcients of the ionogels were measured under ambient conditions using a home-built system,[1,2] which consisted of two Peltier devices (TEC1-19906 by Beijing Geshang Electronic Pte. Ltd.) affixed on an alumina heat sink. The temperature difference (ΔT) across the sample was detected with two T-type thermocouples (Omega, US) which have a diameter of 25 μm, and the thermo-voltage output (ΔV) was measured with a Keithley 2000 multimeter. For each sample, the ΔV values were measured at four different ΔT values. The ionic Seebeck coeffcient of each sample was derived through the best linear fitting of the ΔV-ΔT plots. The Seebeck measurement system was calibrated with a pure nickel foil.

The room-temperature ionic conductivities of the ionogels were measured by the ac impedance spectroscopy with an ECO CHEMIE Autolab system. The samples with the width, length and thickness of 5 mm, 5 mm, and 1 mm, respectively, were sandwiched between two stainless steel electrodes without air gap between samples and electrodes. A spacer was used during the measurement to keep separation between the two electrodes. The frequency was scanned from 0.1 Hz to 100 KHz. The dependence of ionic conductivity on temperature was determined using a CDM 210 Conductivity Meter equipped with a CDC 641 cell and a temperature sensor. The electrochemical behaviors of the ionic supercapacitors were tested with an ECO CHEMIE Autolab system. The voltage scan rate was 20 mV s^{-1} for cyclic voltammetry (CV) measurement, and the frequency was 0.1 Hz to 100 KHz for the electrochemical impedance spectroscopy (EIS).

Transmission electron microscopic (TEM) and scanning electron microscopic (SEM) images were obtained using a field emission electron microscope (JEM-2010F, JEOL) and a field emission scanning electron microscope (Zeiss supra 40), respectively. Dynamic mechanical analyses were performed using an Advanced Rheometric Expansion System (ARES) G2 Rheometer in the dynamic mode with a plate diameter of 20 mm. The Fourier-transform infrared spectra (FTIR) were acquired with a Carry 600 (Agilent Technologies). Attenuated total reflectance FTIR (ATR-FTIR) was performed with a PerkinElmer FTIR spectrometer. The Raman spectra was obtained with a LabRAM HR Evolution (Horiba Scientific). Dynamic light scattering (DLS) measurements were carried out using a Zetasizer Nano ZS by Malvern with a HeNe laser (633 nm) as the light source. The thermal conductivities were

determined by the transient heating method using a TCi Thermal Conductivity Analyzer (C-therm). The ionogel films of 1 mm thick were prepared for measurement. During measurement, a transient heat was supplied to the sample which directly contacted with the sensor surface. The thermal conductivity could be obtained from the temperature response.

For the electrophoretic deposition, 1 wt.% SiO_2 nanoparticles with an average diameter of 20 nm was dispersed in EMIM-DCA. They were stirred for 30 min and then sonicated in an ultrasonic bath for 30 min. Two Pt electrodes were inserted into the sealed electrolytic cell filled with the SiO_2 dispersion in EMIM-DCA. A voltage of 10 V was applied to the two electrodes for 90 min. The surface of the electrodes was examined with a Nikon Eclipse LV 100 optical microscope.

The ionic conductivity (σ) of the ionogels was calculated in terms of the intrinsic resistance R obtained from the intercept of the X-axis at high frequency by fitting an equivalent circuit to the Nyquist plot as shown below,[3] and calculated through the following equation:[4]

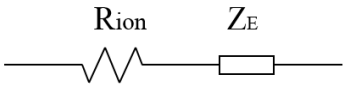

$$\sigma = \frac{1}{R}\frac{L}{Area} \quad (1)$$

where L is the ionogel thickness and $Area$ is the effective electrode area.

The average power of the ionic thermoelectric capacitor during one thermal cycle is calculated based on the following equations:

$$E = \int V_{load} I dt = \int \frac{V_{load}^2}{R_{load}} dt \quad (2)$$

and $$P = \frac{E}{\Delta t} \quad (3)$$

where V_{load} is the voltage across the external load, R_{load} is the resistance of external load, and Δt is the duration of the stage (ii) and (iv) in one thermal cycle.

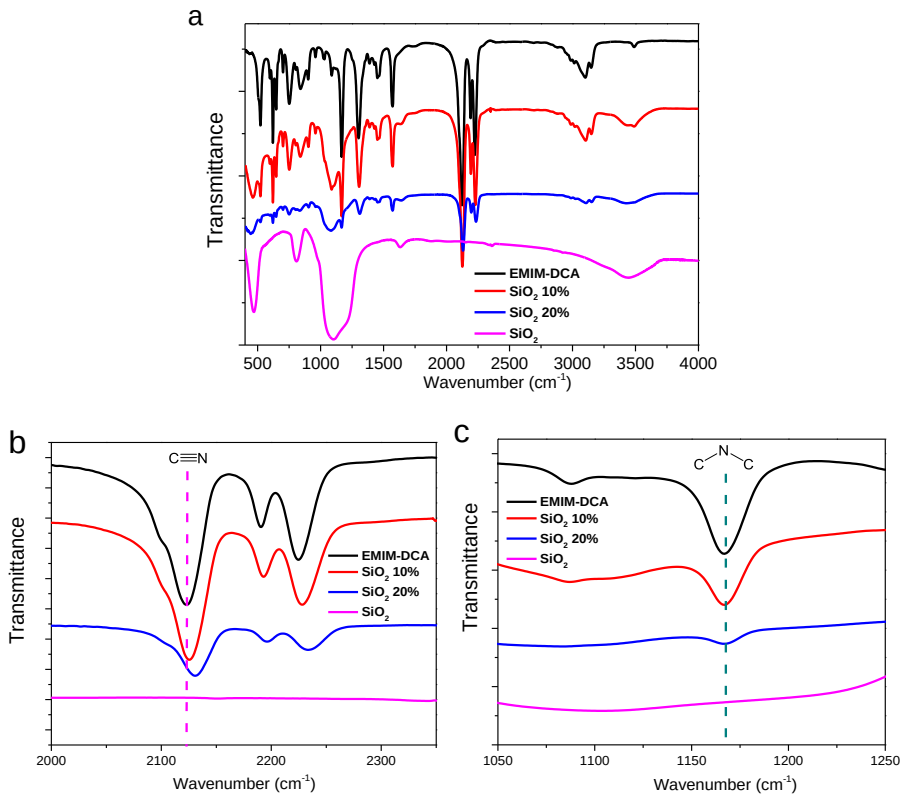

Fig. S1. FTIR spectra of EMIM-DCA, SiO_2 and EMIM-DCA/SiO_2 ionogels with the SiO_2-to-IL mass percentages of 10% and 20% in the wavenumber range of (a) 400-4000 cm^{-1}, (b) 2000-2350 cm^{-1}, and (c) 1050-1250 cm^{-1}.

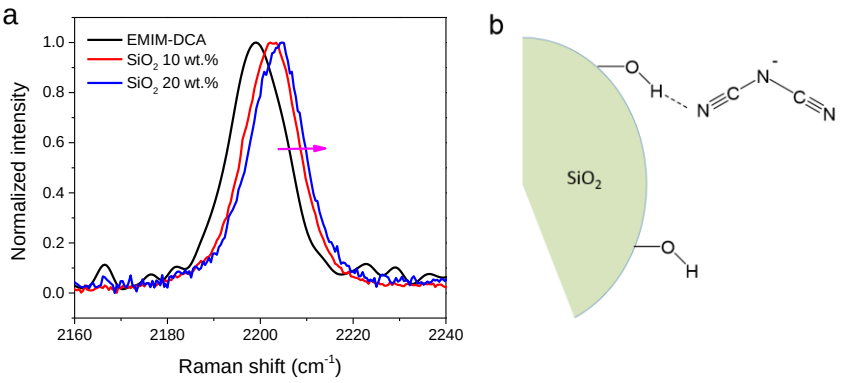

Fig. S2. Raman spectra of EMIM-DCA/SiO_2 ionogels with different SiO_2-to-IL mass percentages. (b) Schematic illustration of the interaction between the surface of a SiO_2 nanoparticle and the anion of EMIM-DCA.

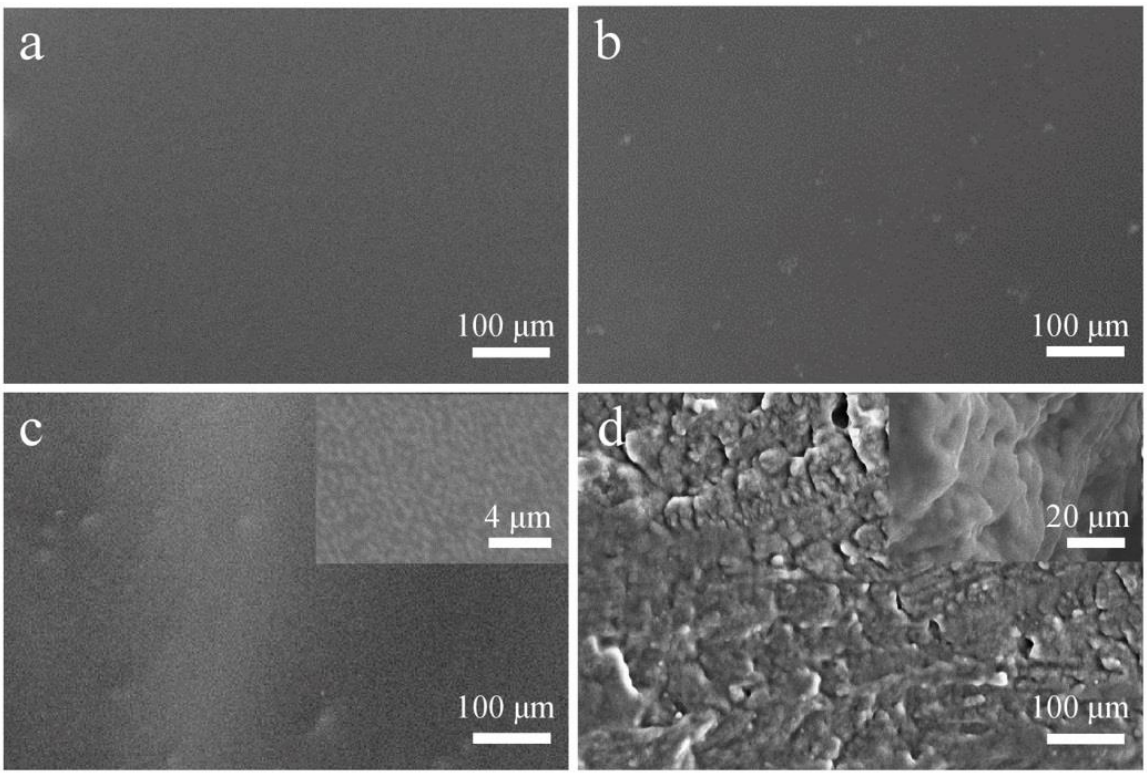

Fig. S3. SEM images of EMIM-DCA/SiOs ionogels with the SiO_2-to-IL mass percentages of (a) 0%, (b) 5%, (c) 20%, and (d) 40%. The average size of SiO_2 nanoparticles is 20 nm.

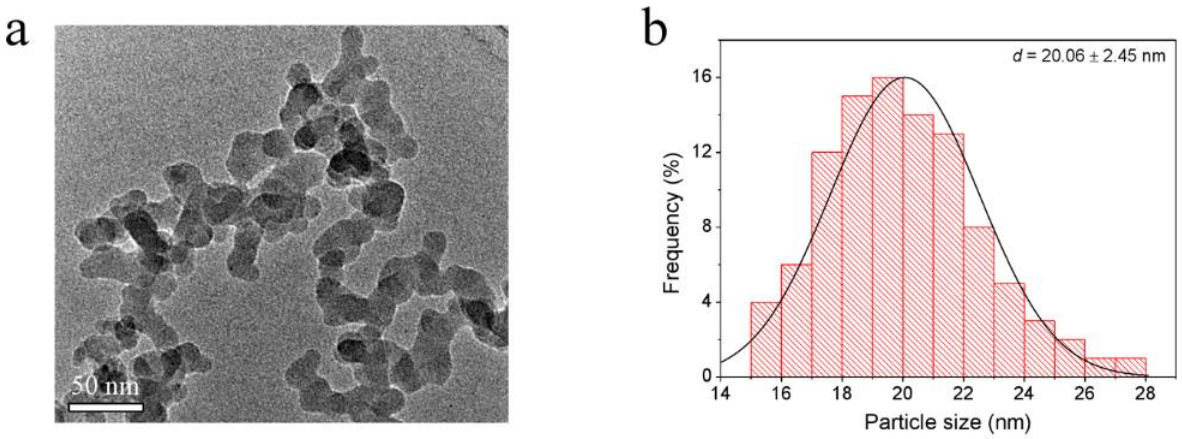

Fig. S4. (a) TEM image and (b) size histogram of the SiO_2 nanoparticles with an average size of 20 nm.

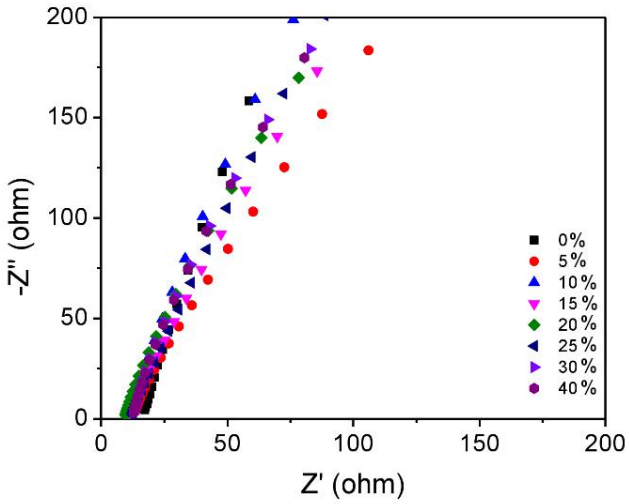

Fig. S5. Nyquist plots of EMIM-DCA/SiO_2 ionogels with the SiO_2-to-IL mass percentages from 0 to 40%. Details for calculation and equivalent circuit are shown in experimental section.

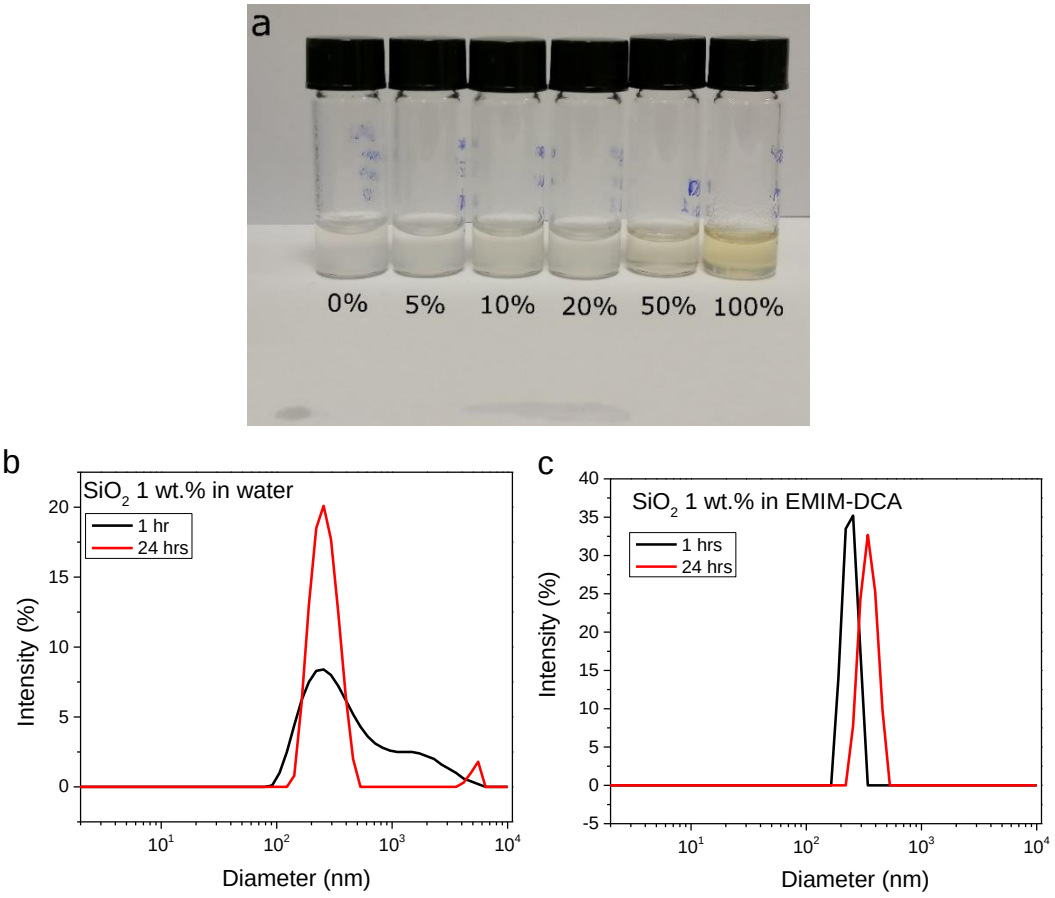

Fig. S6. (a) Stability of 1% SiO_2 nanoparticles in water/EMIM-DCA mixtures with different EMIM-DCA weight loadings after the dispersion of the SiO_2 nanoparticles for 1 hr. Dynamic light scattering results of SiO_2 nanoparticles after dispersed in (b) water and (c) EMIM-DCA for1 hr and 24 hrs.

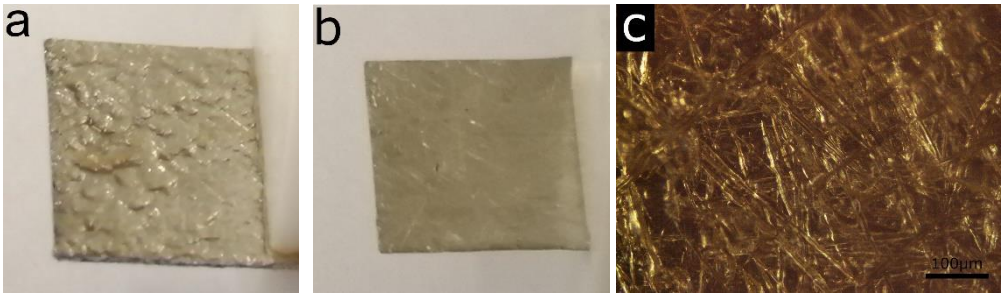

Fig S7. Photo images of (a) positive and (b) negative Pt electrodes after electrophoretic deposition in EMIM-DCA containing 1 wt.% SiO_2. (c) An optical microscopic image of SiO_2 nanoparticles deposited on the positive Pt electrodes.

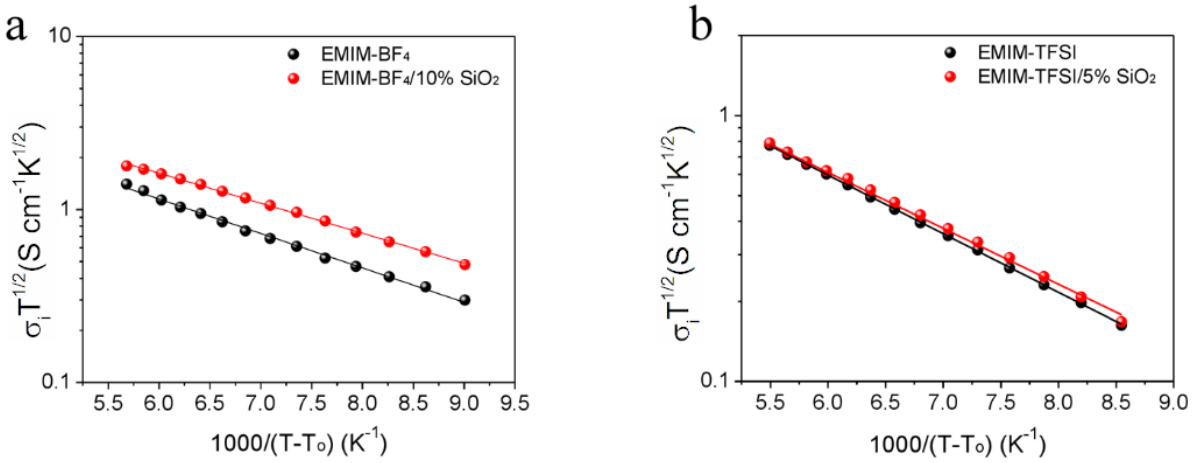

Fig. S8. Temperature dependences of the ionic conductivity of (a) EMIM-BF_4 and EMIM-BF_4/SiO_2 and (b) EMIM-TFSI and EMIM-TFSI/SiO_2 iongels with the optimal SiO_2 nanoparticle loading.

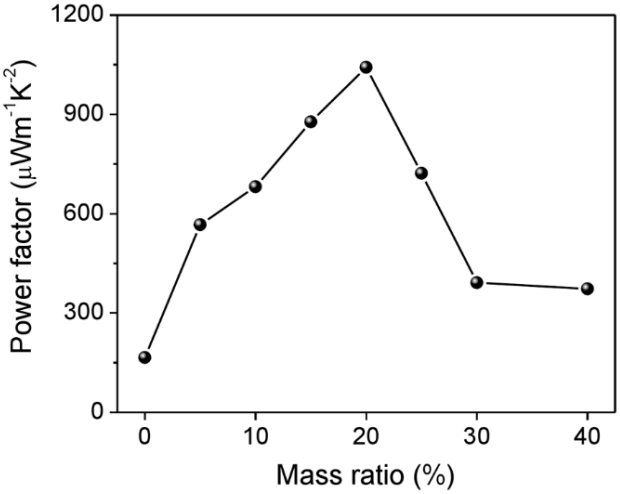

Fig. S9. Variation of the ionic power factor of EMIM-DCA/SiO_2 ionogels with the SiO_2-to-IL mass percentage.

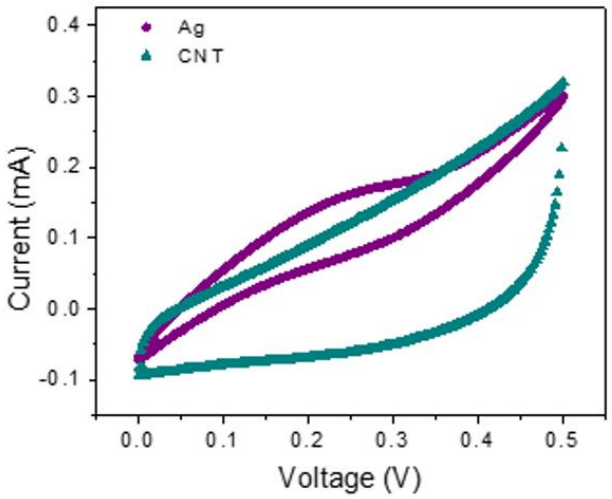

Fig. S10. Cyclic voltammograms of an ITESC with Ag and SWCNT electrodes. The scan rate was 20 mV s^{-1}.

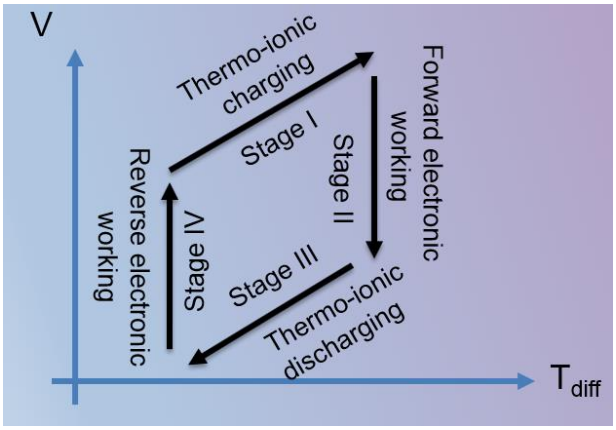

Fig. S11. Heat-to-electricity conversion of an ionic thermoelectric supercapacitor (ITESC) in a full thermal cycle under temperature gradient (ΔT). Stage (i), thermos-ionic charging at open circuit condition and heat on (ΔT). Stage (ii), forward electronic working. An external is connected to the ITESC. Stage (iii), thermos-ionic discharging. The external load is disconnected, and the heat is off. Stage (iv), reverse electronic working. When the external load is re-connected to the ITESC and the heat is remained off, the discharging of the ITESC does work to the external load.

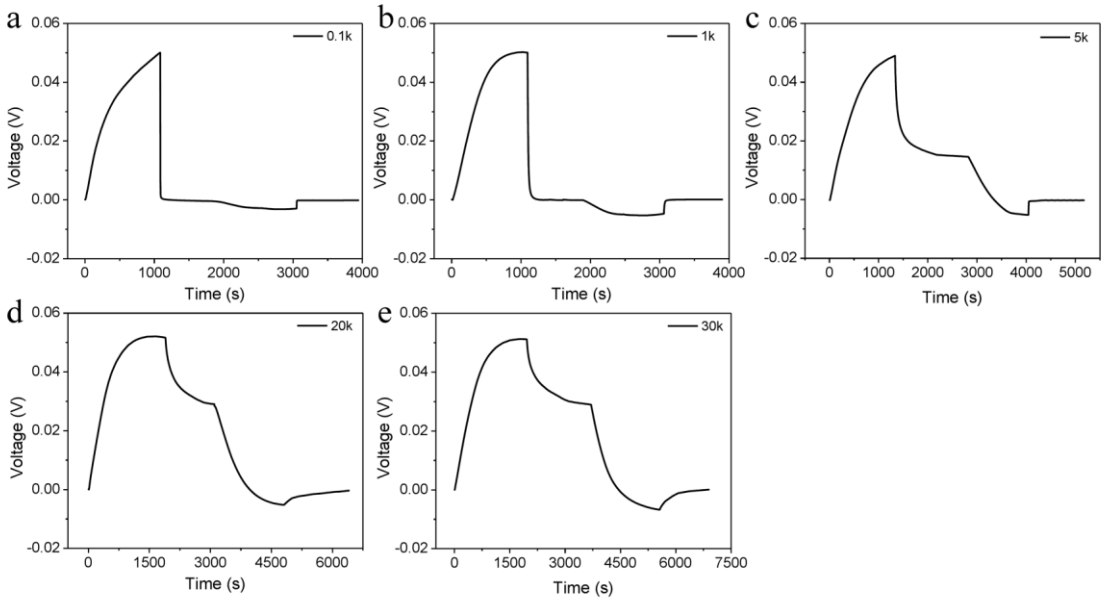

Fig. S12. Voltage profiles of an ITESC with an external load with the resistances of (a) 0.1 kΩ, (b) 1 kΩ, (d) 5 kΩ, (d) 20 kΩ, (e) 30 kΩ.

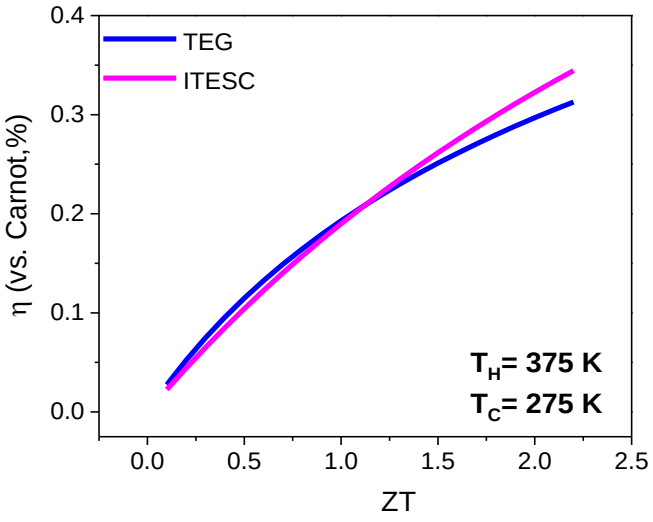

Fig. S13. Variation of the heat-to-electricity conversion efficiency (η) of TEG and ITSEC with ZT. T_H=375 K and T_C= 275K.

Table S1. Appearance of the EMIM-DCA/SiO_2 mixtures with different SiO_2 particle sizes.

SiO_2 particle size	SiO_2-to-IL mass percentage (%)									
	0	5	10	15	20	25	30	35	40	45
7 nm	L	VL	G	G	G	G	P	P	P	P
14 nm	L	VL	G	G	G	G	G	P	P	P
20 nm	L	VL	G	G	G	G	G	G	G	P
30 nm	L	VL	G	G	G	G	G	G	G	G
500 nm	L	L	L	L	L	L	L	L	L	L

L, liquid containing particles; VL, viscous liquid; G, gel; P, particle aggregates

Table S2. Activation energy (E_a) of ionic liquids and ionogels with the optimal SiO_2 loading.

Ionic Liquid/SiO_2 gel	KJ mol^{-1}
EMIM-DCA	4.48
EMIM-DCA/20%SiO_2	3.82
EMIM-BF_4	3.81
EMIM-BF_4/10%SiO_2	3.32
EMIM-TFSI	4.22
EMIM-TFSI/5%SiO_2	4.02

Derivation of the heat-to-electricity conversion efficiency of ionic thermoelectric supercapacitor (ITESC)

The major difference between TEG and our ITESC is that an ITESC can provides intermittent energy generation instead of continuous power supply. Even though, the efficiency can be calculated as ratio between the electric power generated and the heat energy consumption as shown in literature[2,5]. The derivation process is also shown below,

Electrical energy generation (**energy output**):

$$E_e = \frac{1}{2}\frac{Q^2}{C} = \frac{1}{2}C{V_{ion}}^2 \quad (4)$$

E_e is the energy generated in stage ii or iv, (Fig. 4b and S10). Q is the charge needed to balance the ionic potential, C is the electrode/electrolyte (ionogel) capacitance, V_{ion} the thermovoltage from the ionogels.

Since both stages (ii) and (iv) can used for the energy generation, the total electrical energy

generated is:

$$E_{out} = 2E_e = CV_{ion}{}^2 \quad (5)$$

For the heat energy consumption (**energy input**), it can be divided into three parts:

(1) Peltier heat absorption from thermo-current:

$$E_{in}{}^1 = S_i T_H \int Idt \quad (6)$$

Where S_i is the ionic Seebeck coefficient, T_H is the temperature at hot side, I is current through the outer circuit when connecting the external load, t is the duration time to finish the discharge process in stage ii.

(2) Heat that flows along the ITESC to maintain temperature gradient:

$$E_{in}{}^2 = \kappa A \int \Delta T dt \quad (7)$$

Where κ is the thermal conductivity of the ionic conductor (ionogels), ΔT is the temperature gradient during stage ii. A is the area where heat flow crosses.

(3) Joule heating during the current,[6]

$$E_{in}{}^3 = -\frac{1}{2}\int I^2 R dt \quad (8)$$

Where R is the internal resistance and it is assumed highest power can be achieved when external resistance equals external resistance.

Because $\int Idt = Q = CV = CS_i \Delta T$ (9)

and $\int I^2 R dt = C(S_i \Delta T)^2$ (10)

Thus, the total heat consumption should be:

$$E_{in} = C(S_i \Delta T)^2 + \kappa A \Delta T \Delta t_{ii} - \frac{1}{4} C(S_i \Delta T)^2 \quad (11)$$

Where t_{ii} is the discharge time in stage ii. Considering the energy release process in stage ii can be released with 99% during 5τ (time constant τ =CR). Therefore, the efficiency of an ITESC is related to the ionic conductivity and Seebeck coefficient of the ionic conductor as expressed below,

$$\eta = \frac{2\Delta T}{2T_H + \frac{10T\kappa}{\sigma_i S_i{}^2} - \frac{1}{2}\Delta T} \quad (12)$$

By defining the ionic $ZT_i = \sigma_i S_i^2/\kappa$, the relation between the efficiency and ionic Figure of merit of ITESC is shown in below,

$$\eta = \frac{2\Delta T}{T_H} \frac{ZT_i}{2ZT_i + \frac{10T}{T_H} - \frac{1}{2} ZT_i \frac{\Delta T}{T_H}} \quad (13)$$

Therefore, the efficiency difference of ITESC and TE in term of the ZT can be plotted assuming T_H = 375 K and T_c = 275 K as shown in Fig. S13. It is important to note that although there is no more temperature gradient in stage (iii) and stage (iv), both stage (ii) and stage (iv) can be used for electrical energy harvest indicated by the appearance of voltage on the external load.

References

1 Z. Fan, P. Li, D. Du and J. Ouyang, *Adv. Energy Mater.*, 2017, **7**, 1602116.

2 H. Cheng, X. He, Z. Fan and J. Ouyang, *Adv. Energy Mater.*, 2019, **9**, 1901085.

3 E. T. Mcadams, A. Lackermeier, J. A. Mclaughlin and D. Macken, *Biosens. Bioelectron.*, 1995, **10**, 67–74.

4 Q. Li and H. Ardebili, *J. Power Sources*, 2016, **303**, 17–21.

5 H. Wang, D. Zhao, Z. U. Khan, S. Puzinas, M. P. Jonsson, M. Berggren and X. Crispin, *Adv. Electron. Mater.*, 2017, **3**, 1700013.

6 D. M. Rowe, *CRC Handbook of Thermoelectrics*, CRC press, 1995.